

# Dynamics of force-induced DNA slippage

Richard A. Neher and Ulrich Gerland<sup>y</sup>

Department of Physics and CENS, LMU Muenchen, Theresienstrasse 37, 80333 Muenchen, Germany  
(dated: December 30, 2021)

We study the basepairing dynamics of DNA with repetitive sequences where local strand slippage can create, annihilate, and move bulge loops. Using an explicit theoretical model, we find a rich dynamical behavior as a function of an applied shear force  $f$ : reptation-like dynamics at  $f = f_c$  with a rupture time scaling as  $N^3$  with its length  $N$ , drift-diffusion dynamics for  $f_c < f < f_s$ , and a dynamical transition to an unraveling mode of strand separation at  $f = f_s$ . We predict a viscoelastic behavior for periodic DNA with time and force scales that can be programmed into its sequence.

The dynamics of basepairing in DNA and RNA molecules plays an important role in biological processes such as DNA replication, transcription and RNA folding [1]. These dynamics can be probed in detail with modern single molecule techniques to exert and measure piconewton forces with nanometer spatial resolution [2]. For instance, double-stranded DNA (dsDNA) can be forced to open either by pulling on the two strands from the same end of the dsDNA ('unzipping') [3, 4, 5] or from opposite ends ('shearing') [6]. In the case of unzipping, the dynamics involves the consecutive opening of native basepairs, i.e. those present in the ground state of the molecule, and is well understood theoretically [7]. Here, we consider instead the shearing of dsDNA and focus specially on periodic DNA sequences. This case is particularly interesting both from a physical and a biological point of view, since (i) periodic sequences have many non-native basepairing conformations where one strand is shifted with respect to the other, (ii) shearing probes the transitions between such states, i.e. the dynamics of DNA slippage, see Fig. 1, and (iii) DNA slippage during genome replication allows the expansion of nucleotide repeats, and, for certain repeats inside genes, triggers a variety of diseases including Huntington's disease [8].

The mechanism for DNA slippage has already been suggested by Porschke [9], see Fig. 1a: small bulge loops can form at one end of the molecule when a few bases spontaneously unbind and rebind shifted by one or several repeat units. Once formed, a bulge loop may diffuse along the molecule and anneal at the other end, effectively sliding the two strands against each other by a length equal to the size of the bulge loop. This mechanism involves only small energetic barriers compared to the large barrier for complete unbinding and reassociation. Here, we present a detailed theoretical study of force-induced DNA slippage, which has so far not been studied experimentally. We show that this system displays a rich dynamical behavior which can be controlled experimentally by adjusting the force, sequence length, and sequence composition.

**Model.** We consider a dsDNA of two perfectly complementary periodic sequences with  $N$  repeat units, each consisting of  $m$  nucleotides (for simplicity, we refer to re-

peat units also as 'bases'). Assuming that basepairing within a strand is negligible, a basepairing conformation is specified by the set of the  $n$   $N$  inter-strand basepairs  $S = \{f(u_i; l_i)\}$  with  $1 \leq u_1 < u_2 < \dots < u_n \leq N$  for the 'upper' strand and analogously for the  $l_i$  in the 'lower' strand. We assign a binding energy  $\epsilon_b < 0$  to each basepair and a loop cost  $E_l(j) > 0$  when there are  $j > 0$  unpaired bases (total on both strands) between two consecutive basepairs. With a constant shear force  $f$ , see Fig. 1b, the energy of a conformation  $S$  is

$$E[S] = \epsilon_b n[S] + \sum_{i=2}^n E_l(u_i - l_{i-1} - 2) - f L[S]; \quad (1)$$

where  $u_i = u_i - u_{i-1}$  and  $l_i = l_i - l_{i-1}$ . The loop cost  $E_l(j)$  increases with the loop length, starting from  $E_l(0) = 0$ . Free DNA ( $f = 0$ ) is described by  $E_l(j) = \epsilon_l + 3 k_B T \ln(j)$ , with a loop initiation cost  $\epsilon_l > 0$  and a logarithmic asymptotic behavior derived from polymer theory ( $0.6$  is the Flory exponent) [10]. An applied force can affect  $E_l(j)$ , however our qualitative results are insensitive to its precise form [11]. Unless stated otherwise, we keep only the constant term,  $E_l(j) = \epsilon_l$ , for simplicity. The total extension  $L$  is

$$L[S] = \epsilon_s (u_1 - l_1 + N) + \sum_{i=2}^n \min(u_i; l_{i-1}); \quad (2)$$

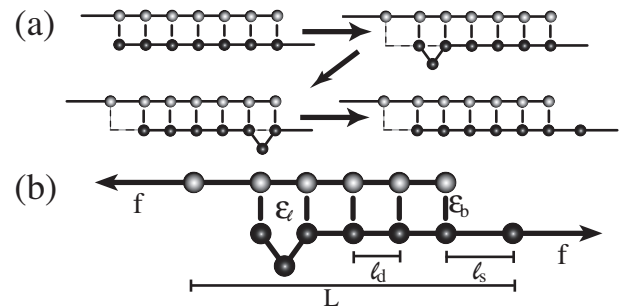


FIG. 1: Sketch of periodic dsDNA, where each bead represents one repeat unit consisting of one or several bases. (a) Many microscopic slippage events can lead to macroscopic sliding. (b) An applied shear force.

where  $\lambda_d$  and  $\lambda_s > \lambda_d$  are the effective lengths (in the direction of the force) per single and double stranded unit, respectively. The entropic elasticity of DNA [12] causes both  $\lambda_d$  and  $\lambda_s$  to depend on the applied force, however since the DNA is almost fully stretched at the forces of interest here, we use the constant values  $\lambda_d = m = 3.4 \text{ \AA}$  and  $\lambda_s = m = 7 \text{ \AA}$  for simplicity [13].

We study the dynamics of our model both with analytical methods (described below) and a Monte Carlo approach using three elementary moves [14]: opening, closing, and slippage of a single basepair, i.e. a pair  $(u_i; l_i)$  is removed from the set  $S$  or added to it, or, if the basepair is adjacent to a loop, either  $u_i$  or  $l_i$  can be changed to another base inside the loop. The absolute timescale of these dynamics is hard to predict, but comparison with bulk reannealing experiments [9] suggests that our simulation time step is on the order of  $\mu\text{s}$  in real time.

**Scaling of mean rupture times.** With a constant applied force  $f > 0$ , eventually every finite dsDNA will rupture, since complete separation of the strands ( $L \rightarrow 1$ ) is the state of minimal free energy. However, both the timescale and the nature of the rupture dynamics depend drastically on the force. Fig. 2 displays the scaling of the mean rupture time  $\tau$  with the number of bases  $N$  for a number of different forces (see caption for parameters). We observe four distinct asymptotic behaviors: an exponential increase with  $N$  for small forces, a cubic scaling with  $N$  at a certain force  $f_c$ , a nearly quadratic scaling above  $f_c$  but below a second threshold  $f$ , and linear scaling above  $f$ . The behavior in the two extremes is easily interpreted: for small  $f$ , rupture is driven by thermal fluctuations across a large free energy barrier with an associated Kramers time that scales exponentially with  $N$ , and linear scaling at large  $f$  is expected when individual bonds break sequentially at a constant rate. We now characterize the rich behavior in the intermediate force regime, including the nature of the two transitions.

The thermodynamic energy barrier disappears at a force  $f_c$  which can be estimated by balancing the binding energy per basepair with the mechanical work exerted when sliding both strands against each other by one step,

$$f_c = \frac{1}{2}(\lambda_s - \lambda_d) : \quad (3)$$

$f_c$  is a critical force in the thermodynamic sense, if the state of complete rupture is excluded (see below for the exact calculation including all basepairing configurations). At  $f = f_c$ , the rupture dynamics is best understood by analogy with the reptation problem [15], since bulge loops in the DNA structure behave similarly to the "stored length" excitations of a single chain in a polymer network: these excitations are generated at the ends of the polymer with constant rate independent of  $N$ , diffuse along the polymer and reach the other end with a probability  $\sim N^{-1}$ . Therefore, the macroscopic diffusion

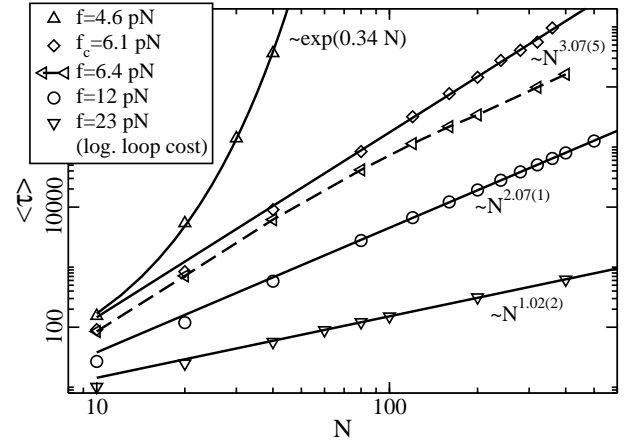


FIG. 2: Scaling of the mean rupture time  $\tau$  with the number of bases  $N$  for different shear forces (with  $\lambda_b = 1:1$ ,  $\lambda_s = 2.8$ , which roughly corresponds to AT-sequences at 50 C, see Fig. 5). The symbols represent Monte Carlo data (error less than symbol size). The solid lines for  $f \leq f_c$  are power law fits (exponent with error in least significant digit is given; data with  $N < 40$  shows significant size deviations and is excluded). For  $f < f_c$  the rupture time increases exponentially. The data for  $f = 6.4 \text{ pN} > f_c$  (connected by the dashed line), demonstrates the crossover from diffusive to drift behavior, see main text. The data for  $f = 23 \text{ pN}$  is calculated including the logarithmic loop cost, which becomes relevant at large forces [11].

constant for the relative motion of the two DNA strands should scale as  $D \sim N^{-1}$  and the time for diffusion over distance  $N$  is  $\sim N^3$ .

For  $f > f_c$  strand separation is energetically a downhill process, which induces a drift velocity  $v$  between the two strands. In linear response, we expect  $v = f$  for small  $f = f_c$  with a mobility mediated by bulge loop diffusion,  $\mu = D/k_B T \sim N^{-1}$  (from the Einstein relation), leading to  $\tau \sim N^2$ . Why does this behavior not persist for large forces? The second transition in the scaling behavior is due to a change in the rupture mode: at forces larger than  $f = \frac{1}{2}(\lambda_s - \lambda_d)$  the double strand can open by unraveling from both ends, i.e. the energy cost  $\lambda_b$  of opening a basepair at the end is outweighed by the gain  $f(\lambda_s - \lambda_d)$  from a longer base-to-base distance in the single strand. In this unraveling mode, the rupture time scales linearly with  $N$ . The dynamical transition from sliding to unraveling is clearly reflected in the length at rupture,  $L [S(\cdot)]$ , see Fig. 3a, which is roughly a factor of two larger for sliding.

**Rupture time distributions.** Single molecule setups are ideally suited to record the full distribution of rupture times,  $P(\cdot)$ , which is a sensitive characteristic of the dynamics and permits a close examination of the physical picture introduced above. The histograms in Fig. 4 show  $P(\cdot)$  from simulations at  $f = f_c$  and a larger force  $f_c < f < f$ , see caption for parameters. We observe that fluctuations play a dominant role at  $f = f_c$ , i.e. the width of  $P(\cdot)$  is comparable to the mean, while the rup-

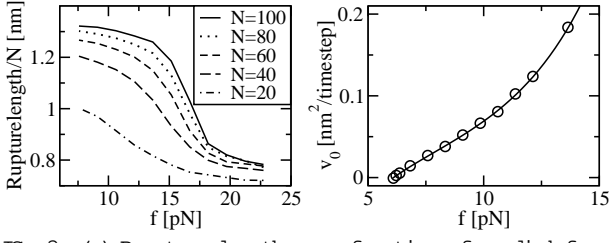


FIG. 3: (a) Rupture length as a function of applied force  $f$  (parameters as in Fig. 2). (b) Drift coefficient  $v_0(f)$  extracted from simulations with  $N = 150$  (circles) and analytical curve (solid line,  $k_0 = 1.87$ ), see main text.

ture dynamics is drift dominated at the larger force, with a localized peak in  $P(x)$ .

To formulate the drift-diffusion dynamics quantitatively, we treat the number of bases in the double-stranded region as a continuum variable  $x$  with  $0 < x < N$ , and consider the probability distribution  $P(x;t)$ , which satisfies the continuity eq.  $\partial_t P(x;t) = -\partial_x j(x;t)$  with a force-dependent current

$$j(x;t) = -D(f;x) \partial_x P(x;t) - v(f;x) P(x;t) : \quad (4)$$

The above discussion suggests a diffusion coefficient of the form  $D(f;x) = D_0(f)/x$  and similarly a drift  $v(f;x) = v_0(f)/x$ . We have an absorbing boundary at  $x = 0$  and it is natural to choose a reflecting boundary at  $x = N$  and a delta peak at  $x = N$  as initial condition. The solution  $P(x;t)$ , which must in general be obtained numerically, determines the rupture time distribution through  $P(x) = j(0;)$ .

We can determine the force-dependence of the diffusion coefficient and drift empirically by fitting the calculated  $P(x)$  to the simulation data using  $D_0$  and  $v_0$  as adjustable parameters. The solid lines in Fig. 4 show that the drift-diffusion theory describes the simulation data well. Fig. 3b shows the fitted  $v_0$  as a function of  $f$  (circles). The drift vanishes at the critical force,  $v_0(f_c) = 0$ , confirming the physical picture. The drift-diffusion theory also explains the crossover behavior in the vicinity of  $f = f_c$ , see Fig. 2: the drift is significant only when the system size  $N$  is larger than the diffusive length  $D_0 = v_0$  [16]. Hence, with  $v_0 \propto 1/f$ , reptation-like dynamics is expected in a force interval  $f \propto N^{-1}$  around  $f_c$ .

Microscopic dynamics. Next, we study how the macroscopic drift in eq. (4) emerges from the microscopic bulge loop dynamics and determine  $v_0(f)$  in terms of our system parameters. Since bulge loops on opposite strands annihilate each other when they meet, the bulge loop dynamics is equivalent to a reaction-diffusion system of particles and antiparticles in one dimension. Both particles and antiparticles are created at each end, however with different rates determined by the applied force. From the underlying master equation for these processes one

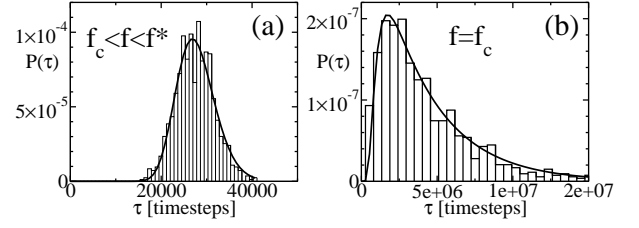


FIG. 4: Histogram of rupture times for two different forces, (a) 34.4 pN and (b)  $f_c = 16.6$  pN, but the same set of DNA parameters,  $N = 80$ ,  $b_b = 3/75$ ,  $\epsilon_b = 2/6$ , which roughly correspond to a CG-sequence at room temperature, see Fig. 5.

obtains the mean-field equations [11]

$$\begin{aligned} \partial_t u(y;t) &= k_0 \partial_y^2 u(y;t) - k_1 u(y;t) l(y;t) + k_2 ; \\ \partial_t l(y;t) &= k_0 \partial_y^2 l(y;t) - k_1 u(y;t) l(y;t) + k_2 ; \end{aligned} \quad (5)$$

where  $u(y;t)$  and  $l(y;t)$  denote the bulge loop density on the upper/lower strand,  $y \in [0;x]$  is the position within the double stranded region, and  $k_0, k_1, k_2$  are the rates for hopping, annihilation, and pair creation, respectively. At the boundaries, the densities take on constant values,  $u(0;t) = l(x;t) = \langle \cdot \rangle$  and  $u(x;t) = l(0;t) = \langle \cdot \rangle$ , where  $\langle \cdot \rangle(f)$  and  $\langle \cdot \rangle(f)$  are calculated below by assuming a local equilibrium of the DNA at the edges. The macroscopic drift is determined by the stationary solution and depends only on the difference between the loop densities on the upper/lower strand,  $v(f;x) = k_0 \partial_y [u(y) - l(y)]$ . Using eq. (5) this yields  $v_0(f) = 2k_0 [\langle \cdot \rangle(f) - \langle \cdot \rangle(f)]$ . Fig. 3b shows that this result is in excellent agreement with the empirical  $v_0(f)$  obtained above.

Since the loop cost  $E_b(j)$  is larger for two separate loops than for a single one of the combined length, bulge loops on the same strand feel a short-range attraction. However, the interaction is not strong enough to cause a significant aggregation of the loops in our Monte Carlo simulations. This is consistent with the observation that with our DNA parameters, the interaction energy  $\epsilon_b$  is never significantly larger than the entropic cost  $-\log$  of colocalization at loop density  $\rho$ . While  $v_0(f)$  is apparently robust to interaction effects, the diffusion coefficient  $D_0(f)$  is sensitive to interactions as well as correlations. Both are neglected in eq. (5), leaving the microscopic calculation of  $D_0(f)$  as a challenge for the future.

Critical force. To obtain the exact critical force, we need the partition function  $Z = \sum_S e^{-E(S)/k_B T}$  summed over all configurations  $S$  with at least one basepair. It is useful to allow for different numbers of bases in the two strands, e.g.  $1 \leq u \leq N$  and  $1 \leq l \leq M$ , with a corresponding partition function

$$Z(N;M) = \sum_{i=0}^{N-1} \sum_{j=0}^{M-1} b_s^{i+j} Z_p(n;m) ; \quad (6)$$

where  $b_s = e^{\epsilon_s/k_B T}$  is the Boltzmann factor for a stretched base, and  $Z_p(n;m)$  is the partition function for

Sequence		20 °C	37 °C	50 °C
AA....	$\epsilon_b$	2.37	1.62	1.11
TT....	$\epsilon_l$	4.16	3.1	2.8
CC....	$\epsilon_b$	3.75	2.98	2.46
GG....	$\epsilon_l$	2.6	3.5	4.16
CAGCAG....	$\epsilon_b$	10.5	8	6.36
GTCGTC....	$\epsilon_l$	11.8	10.9	10.2

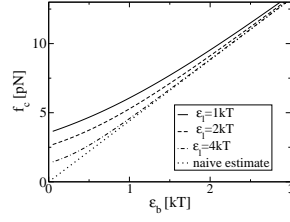


FIG. 5: (a) Model parameters for different DNA sequences and temperatures as obtained by fitting to a detailed thermodynamic model [11, 17] (all energies in units of  $kT$ ). (b) The exact critical force compared to the estimate of eq. (3).

the central, double stranded section starting with the first and ending with the last basepair, cf. Fig. 1b. We calculate  $Z_p(n; m)$  recursively by introducing a complementary partition function  $Z_u(n; m)$  containing only structures where the last of the  $n$  upper bases is not bound to the last of the  $m$  lower bases:

$$\begin{aligned}
 Z_p(n+1; m+1) &= q_b Z_p(n; m) + q_b g Z_u(n; m); \quad (7) \\
 Z_u(n+1; m+1) &= g \sum_{k=1}^n Z_p(k; m+1) + g \sum_{k=1}^m Z_p(n+1; k) \\
 &\quad + g_b Z_p(n; m) + b_l Z_u(n; m);
 \end{aligned}$$

Here, the Boltzmann factors  $q = e^{-\epsilon_b/k_B T}$ ,  $g = e^{-\epsilon_l/2k_B T}$ , and  $b_l = e^{-\epsilon_l/k_B T}$  account for basepairing, loop costs, and stretching of double strand, respectively. These recursion relations allow the efficient calculation of the partition function for finite  $N, M$ . To obtain the critical behavior for  $N \rightarrow \infty$ , we take the  $z$ -transform  $\hat{Z}(z; y) = \sum_{N, M} Z(N; M) z^N y^M$ . The inverse  $z$ -transform is then determined by the simultaneous poles of  $\hat{Z}(z; y)$  in  $z$  and  $y$ , and for large  $N$  the pair of poles with the smallest  $|zy|$  dominates. A detailed analysis of the critical behavior will be presented elsewhere [11]; here we are interested in  $f_c$ , i.e. the force where the dominant pole switches. We find that  $f_c$  is the nontrivial root of

$$\frac{b_s^2}{b_l} q - \frac{b_s^2}{b_l} - 1 - g^2 q \frac{2}{b_s} \frac{b_s^2}{b_l} + 1 = 0; \quad (8)$$

When  $b_l$  or  $b_s \rightarrow k_B T$ , the second term is negligible and the nontrivial root of (8) is  $b_s^2/b_l = q$ , recovering the naive estimate (3). However, for smaller  $b_l, b_s$ , one finds significant deviations from (3), see Fig. 5.

Loop densities. Using the same approach as for the calculation of  $f_c$ , we can calculate the loop densities  $\langle \dots \rangle$  introduced above. Assuming local equilibrium at the edges, i.e. equilibration between all possible conformations of the two strands with a fixed central basepair, we find  $\langle a \rangle = \sum_{a, b} P(a; b) a$  and  $\langle b \rangle = \sum_{a, b} P(a; b) b$ , where  $\langle a \rangle = m \ln(a; b) + 1$  and  $P(a; b) = b_s^{b-a} b_l q g Z_p(N-b-1; N-b-1) / Z(N; N)$ . The sums can be evaluated exactly for large  $N$  [11].

Conclusions. We find a response of periodic dsDNA to shear forces that is very distinct from that for nonperiodic sequences. Above a thermodynamic critical force  $f_c$ , but below a dynamic critical force  $f$ , bulge loop diffusion allows periodic DNA to open by sliding. This mechanism leads to a much lower thermodynamic critical force than the unraveling mechanism by which nonperiodic DNA opens. Within our model, we have calculated  $f_c$  exactly and characterized the associated dynamics, which is effectively viscoelastic with a creep compliance  $\propto N^{-1}$  for  $f_c < f < f$ . Above  $f$  periodic dsDNA also opens predominantly by unraveling (this dynamical transition may be regarded as a remnant of the thermodynamic transition for nonperiodic sequences). Interestingly, periodic DNA could be used as a viscoelastic nanomechanical element with properties that are programmable by choosing sequence length and composition. This may lead to applications in microstructured devices, similar to the programmable DNA-based force sensors reported in Ref. [18].

We thank T. Hwa, F. Kuhner, and M. Rief for fruitful discussions and the DFG for financial support.

- 
- Electronic address: Richard Neher@physik.uni.de  
 Electronic address: Ulrich Gerland@physik.uni.de
- [1] B. Alberts et al., Molecular Biology of the Cell (Garland, New York, 2002).
- [2] C. Bustamante, J.C. Macosko, and G.J. White, Nature Rev. Mol. Cell Biol. 1, 130 (2000). H. Clausen-Schaumann, M. Seitz, R. Kautbauer, H.E. Gaub, Curr. Opin. Chem. Biol. 4, 524 (2000). R. Merkel, Phys. Rep. 346, 343 (2001). R. Lavery, A. Lebrun, J.-F. Allard, D. Bensimon, V. Croquette, J. Phys. Cond. Matter 14, R383 (2002).
- [3] C. Danilowicz et al., PNAS 100, 1694 (2003).
- [4] R. Kautbauer, M. Rief, and H.E. Gaub, Nano Lett. 3, 493 (2003).
- [5] U. Bockelmann, B. Essevaz-Roulet, and F. Heslot, Phys. Rev. E 58, 2386 (1998).
- [6] T. Strunz, K. Oroszlán, R. Schafer, and H.-J. Guntherodt, PNAS 96, 11277 (1999).
- [7] D.K. Lubensky and D.R. Nelson, Phys. Rev. Lett. 85, 1572 (2000); Phys. Rev. E 65, 031917 (2002).
- [8] S.T. Lovett, Mol. Microbiol. 52, 1243 (2004). L.S. Kaplan et al., Biochemistry 42, 2166 (2003).
- [9] D. Porschke, Biophys. Chem. 2, 83 (1974).
- [10] T. Hwa, E. Marinari, K. Sneppen, and L. Tang, PNAS 100, 4411 (2003).
- [11] R. Neher and U. Gerland, to be published.
- [12] S.B. Smith, Y. Cui, and C. Bustamante, Science 271, 795 (1996).
- [13] Here we assume the B-DNA form. Before melting, DNA with a high CG-content undergoes a transition to a stretched S-DNA form at large forces. This transition was found to be rapid compared to melting [H. Clausen-Schaumann et al., Biophys. J. 78, 1997 (2000)], so that S-DNA could be treated by different effective parameters.

- [14] C. Flamm, W. Fontana, I. Hofacker, and P. Schuster, RNA 6, 325 (2000).
- [15] P.-G. de Gennes, J. Chem. Phys. 55, 572 (1971).
- [16] D. K. Lubensky and D. R. Nelson, Biophys. J. 77, 1824 (1999).
- [17] M. Zuker, Nucleic Acids Res. 31, 3406 (2003).
- [18] C. A. Brecht et al., Science 301, 367 (2003).